Microstructural and Phase Evolution of Compound Layers Growing on α–Iron During Gaseous Nitrocarburizing

T. WOEHRLE, A. LEINEWEBER, and E.J. MITTEMEIJER

The microstructural evolution of compound layers grown on 1-mm thick α-iron substrates after nitrocarburizing at 853 K (580 °C) in NH$_3$/H$_2$/N$_2$/CO gas mixtures was investigated by light optical microscopy and X-ray diffraction. The evolution of the microstructure can be divided into several stages. Starting with the formation of the carbon-rich phase cementite, which practically does not contain nitrogen, the phase constitution of the compound layer develops through successive stages of microstructural change into the direction of the nitrogen-richer and carbon-poorer phases ε and γ'. These results are the consequences of (1) the kinetics of nitrogen and carbon uptake at the gas–solid interface and the considerably different solubilities of nitrogen and carbon in the α-iron substrate and (2) the occurrence of local equilibrium conditions prevailing at the solid–solid interphase boundaries in the compound layer. The change of the microstructure as a function of depth in the compound layer is shown to be compatible with so-called "diffusion paths" in the ternary Fe-N-C phase diagram.

I. INTRODUCTION

DIFFUSION-CONTROLLED phase transformations in multicomponent solid-state systems are of great technological importance in a wide range of applications including diffusion bonding, solder joints, welded alloys, microelectronic devices, and the thermochemical surface treatments. All these technologies are based on the modification and (meta)stability of microstructures induced by directional long-range diffusion and chemical reactions at the surface and/or the interfaces of intimately connected phases; therefore, the properties of multicomponent materials can be varied greatly.[1,2] The driving forces for diffusion in such heterogeneous systems are the gradients of the chemical potentials of the components in the reaction zone. If the rate of diffusion is slow compared with the rate of reaction, i.e., the rate of reaction is controlled by the rate of diffusion, so-called local thermodynamic equilibria can be assumed to prevail at the solid–solid phase interfaces in the reaction zone.[3–5] The establishment of local equilibria implies a continuous variation of the chemical potentials of the components through the reaction zone, associated with the possible formation of (one or more) phases within the reaction zone. The sequence and composition of these phases then is described by a so-called diffusion path in (the isothermal section of) the corresponding phase diagram.[3,4,6,7] At a given temperature and pressure, the diffusion path is defined by the course of the average composition in a direction perpendicular to the original interface of the diffusion couple.[4,8] The course of a diffusion path is governed by both the thermodynamics and the kinetics of the interacting components of the system considered.

In the field of thermochemical surface treatments, an important case of (usually) diffusion-controlled phase transformations is met in nitrocarburizing, where nitrogen and carbon are supplied simultaneously to the surface of ferritic iron-based workpieces at temperatures usually between 773 K and 853 K (500 °C and 580 °C).[9–11] If the chemical potentials of nitrogen and carbon imposed by the nitrocarburizing agent are sufficiently high, a compound layer typically composed of iron (carbo)nitrides such as ε-Fe$_3$(N,C)$_{1+x}$ and γ'-Fe$_4$(N,C)$_{1-z}$ develops ([possibly] eventually; see the results presented subsequently) at the surface of the workpiece.[12–14] Under certain nitrocarburizing conditions, also θ-Fe$_3$C (cementite) can form as an additional phase[11] or even as the only phase[15] in the compound layer. The composition ranges of the relevant Fe-N-C phases are given in Table I. Note that in particular, the ε phase exhibits a wide range in composition.

The compound layer (of thickness up to several 10 μm) that grew as a result of nitrocarburizing can lead to a significant improvement of mechanical (resistance to wear and friction) and chemical (resistance to corrosion) properties of the workpiece.[18,19] Underneath the compound layer, the so-called diffusion zone forms, where nitrogen and carbon are dissolved interstitially in the ferritic matrix. The diffusion zone is usually up to several 100 μm thick and induces a considerable improvement in fatigue resistance.[20,21]

Although several investigations on compound-layer development on pure α-iron substrates after nitrocarbu-

T. WOEHRLE, Ph.D. Student, and A. LEINEWEBER, Doctor and Staff Scientist, are with the Max Planck Institute for Intelligent Systems (formerly the Max Planck Institute for Metals Research), Heisenbergstraße 3, D-70569 Stuttgart, Germany. Contact e-mail: a.leineweber@is.mpg.de E.J. MITTEMEIJER, Professor, is with the Max Planck Institute for Intelligent Systems (formerly the Max Planck Institute for Metals Research), and with the Institute for Materials Science, University of Stuttgart, D-70569 Stuttgart, Germany.
Manuscript submitted June 7, 2011.
Article published online April 5, 2012.

rizing have been performed,[11,22–25] a systematic and general description of the compound-layer evolution is still lacking, undoubtedly because of the complexity of the occurring microstructures that are far more complicated than in the case of pure nitriding.

Previous studies on the microstructural evolution of the compound layer growing on pure α-iron substrates after salt-bath nitrocarburizing at 853 K (580 °C)[22] and after gaseous nitrocarburizing at 848 K (575 °C)[23] and 853 K (580 °C)[24] reported the initial formation of Fe₃C (cementite) at the surface of the substrate, which was followed by the subsequent formation of the nitrogen-rich ε-phase. For prolonged treatment times, the compound layer was composed only of (1) both ε and γ'[22,23] or (2) γ'.[24] The initial nucleation of cementite at the substrate surface was explained as a consequence of a much faster absorption rate of carbon than that of nitrogen at the initial stage of nitrocarburizing, implying that the solubility limit of carbon in ferrite is reached faster than that of nitrogen.[22,23]

The current work aims to investigate systematically, by performing dedicated experiments with specifically prepared specimens (Section II), the observed initial formation of the carbon-rich phase cementite at the surface of the α-iron substrate after nitrocarburizing as well as the subsequent evolution of the compound layer. It will be shown that all different microstructures occurring successively *within* the developing compound layer (Section III) can be understood on the basis of local thermodynamic equilibria at the interfaces between the solid phases formed (cf. Section IV). In particular, the relatively high nitrogen solubility in ferrite compared with that of carbon in ferrite is shown to have an important impact on the microstructure of the developing compound layer.

II. EXPERIMENTAL

Rectangular specimens of dimensions $20 \times 25 \times 1$ mm³ were cut from cold-rolled cast iron plates (Alfa Aesar, Ward Hill, MA; 99.98 wt pct), ground, polished (final stage, 1-μm diamond suspension), cleaned ultrasonically in ethanol, and recrystallized in hydrogen for 2 hours at 973 K (700 °C), followed by slow cooling. Immediately before nitrocarburizing the specimens were polished (final stage, 1-μm diamond suspension) and cleaned with ethanol.

Nitrocarburizing experiments were performed at 853 K (580 °C) in a vertical quartz-tube furnace measuring 28 mm in diameter. The process temperature was controlled within ±1 K in the middle of the furnace, where the specimen was placed. The nitrocarburizing atmosphere was composed of NH₃ (99.999 vol pct) as nitriding species, CO (99.997 vol pct) as carburizing species, and H₂ (99.999 vol pct) and N₂ (99.999 vol pct) as inert gases (all gases from Westfalen AG, Münster, Germany). The flow rate of each gas component was adjusted separately by mass-flow controllers. To avoid significant (thermal) dissociation of ammonia and possible side reactions in the gas atmosphere (but see footnote to Table II), which would affect the composition of the gas mixture, a constant overall gas-flow rate

Table I. Composition Ranges and Crystal Structure of Some Relevant Phases in the Ternary System Fe-N-C at a Temperature of 853 K (580 °C)[16,17]

Phase	Crystal Structure	N Content (at. pct)	C Content (at. pct)
α-Fe	Fe: Body-centered-cubic type, N and C in octahedral interstices	0 to 0.37	0 to 0.02
γ'-Fe₄N₁₋$_z$*	Fe: Face-centered cubic-type, N ordered in octahedral interstices	19.4 to 20	<0.7
ε-Fe₃(N,C)₁₊$_x$*	Fe: Hexagonal close-packed-type, N ordered in octahedral interstices	15 to 33	0 to 8
θ-Fe₃C*	Fe: Complicated orthorhombic, C in bicapped trigonal prisms	~0	25

*These phases are metastable with respect to the decomposition into iron and nitrogen and/or carbon.

Table II. Composition of the Nitrocarburizing Atmosphere, the Corresponding Nitriding Potential* $r_N = P_{NH_3}\big/ P_{H_2}^{3/2}$ and Treatment Time Used for Experiments of Series A, B, and C at 853 K (580 °C)

Series	Treatment Time (h)	NH₃ (vol pct)	H₂ (vol pct)	CO (vol pct)	N₂ (vol pct)	r_N (atm$^{-1/2}$)
A	4	13.23	57.95	20	8.82	0.30
	4	15.44	57.95	20	6.61	0.35
	4	17.64	57.95	20	4.41	0.40
	4	22.05	57.95	20	–	0.50
B	0.25	15.44	57.95	20	6.61	0.35
	0.5	15.44	57.95	20	6.61	0.35
	2	15.44	57.95	20	6.61	0.35
	4	15.44	57.95	20	6.61	0.35
	8	15.44	57.95	20	6.61	0.35
	24	15.44	57.95	20	6.61	0.35
C	4	13.23	57.95	20	8.82	0.30

*The nitriding potential is related to the chemical potential of nitrogen in a NH₃/H₂-containing gas mixture,[12] and it determines at a given temperature the iron-nitride phase in equilibrium with a purely nitriding atmosphere. In contrast to the nitriding potential, no defined carburizing potential can be given for the NH₃/H₂/CO/N₂ gas mixtures as applied in the current work because the carburizing potential is hypothetically infinite.[12,15] However, an "effective" carburizing potential prevails on nitrocarburizing because of the side reactions in the gas atmosphere.[26]

of 13.5 mm seconds^{-1} through the quartz tube (calculated for the gas volume at room temperature) was chosen. After nitrocarburizing, the specimens were quenched by dropping them out of the furnace into nitrogen-flushed water.

To investigate the microstructural evolution of the compound layer after nitrocarburizing, two series of experiments were performed in $NH_3/H_2/N_2/CO$ gas mixtures at 853 K (580 °C): (1) using a constant treatment time of 4 hours and a variable gas composition (cf. Table II; series A) and (2) using a variable treatment time and a constant gas composition (cf. Table II; series B).

Additionally, experiments were performed using wedge-shaped specimens obtained by dedicated grinding of original $20 \times 25 \times 1$ mm^3 specimens, which led to a linear thickness variation from 1 mm to 0.02 mm. Using such specimens and the normal rectangular $20 \times 25 \times 1$ mm^3 specimens that were presaturated with nitrogen, the influence of nitrogen saturation of the ferrite substrate on the microstructural evolution of the compound layer could be revealed. The wedge-shaped specimens as well as the nitrogen-presaturated rectangular specimens were nitrocarburized in a (relatively) strongly carburizing atmosphere (cf. Table II; series C).* The nitrogen presaturation was achieved by

---

*The nitrocarburizing atmosphere used for series C leads to the formation of a single-phase cementite layer on 1-mm-thick, rectangular, nonsaturated α-iron substrates.[15,26]

---

nitriding of the rectangular iron specimens for 66 hours at 853 K (580 °C) in a NH_3/H_2 gas mixture containing 10.9 vol pct NH_3 and 89.1 vol pct H_2. These nitriding parameters had been chosen such that a maximum solubility of nitrogen in ferrite was obtained without forming an iron-nitride compound layer.[27] After nitriding, X-ray diffraction was applied to verify that iron nitrides had not formed. The total nitrogen content in the presaturated substrate was determined by weighing the specimen before and after nitriding[28] using a Toledo UMX2 high-precision balance (Mettler-Toledo International, Inc., Columbus, OH). The nitrogen content in the presaturated samples was approximately 0.37 at. pct, which is close to the nitrogen-solubility limit in ferrite at 853 K (580 °C); these data are reported in the literature as approximately 0.36 to 0.38 at. pct.[17,29]

The nitrocarburized specimens were cut into two pieces, which were used for optical microscopy and X–ray powder diffraction, respectively.

The specimens for optical microscopy analysis were covered with an electrodeposited nickel layer using a Watts bath[13] at 333 K (60 °C) to prevent damage of the compound layer during sample preparation. Embedding (Polyfast; Struers GmbH, Willich, Germany) was followed by grinding, polishing (final stage 1 μm diamond suspension), and etching in 1 vol pct Nital containing 0.1 vol pct HCl.[30] Some cross sections were treated additionally with a Groesbeck reagent[31] (4 g KMnO₄,

1 g NaOH, and 1 g KOH per 100 mL H_2O) at 333 K (60 °C), which allows phase identification by discriminative staining of the carbon-containing phases ε-Fe$_3$(N,C)$_{1+x}$ and, in particular, cementite (Fe$_3$C). The γ' phase remains unstained because of the low solubility of carbon, as indicated in Table I. Optical microscopy was performed on cross sections of specimens using a Zeiss Axiophot microscope (Carl Zeiss, Oberkochen, Germany).

X-ray diffractograms for identification of the phases present in the compound layer were recorded from the surface region of the compound layers using a PANalytical X'Pert Multi-Purpose Diffractometer (PANalytical, Almelo, the Netherlands) equipped with a graphite monochromator in the diffracted beam (Co-K$_\alpha$ radiation) and Bragg-Brentano geometry. To obtain better crystallite statistics, the samples were rotated around their surface normal during the measurement.

Microhardness measurements (micro-Vickers) on the specimen cross section were carried out in the ferrite substrate directly underneath the compound layer using a Leica VMHT MOT micro-indentation system (Leica AG, Wetzlar, Germany) with a load of 50 gf ($\cong$0.49 N) and a dwell time of 10 seconds (higher loads occasionally caused localized cracking of the compound layer). Each hardness value presented is an average value of four measurements. The nitrogen content in ferrite (not well measurable with electron probe microanalysis; note the small nitrogen-solubility limit in ferrite of approximately 0.36 at. pct at 853 K [580 °C][17]) was determined using a linear dependence of hardness on nitrogen content in ferrite as reported in Reference 32. The same experimental conditions as described in Reference 32 were used in the current work to ensure the applicability of the reported dependence of hardness on nitrogen content in ferrite.

III. RESULTS

In the following, a shorthand notation for the specification of the microstructure of the compound layer is introduced. For this notation, the compound layer is divided into separate *sublayers* perpendicular to the surface normal, where each sublayer comprises a laterally homogeneous phase constitution, at least over a lateral distance of several 10 μm. In ternary systems (as the Fe-N-C system) at a constant temperature and pressure, a sublayer comprising a (depth) range in composition can be composed either of a single phase or of two different phases (single-phase or dual-phase sublayers) if the phase rule is obeyed. The overall phase constitution of the compound layer can then be denoted by the sequence of sublayers (separated by "/"), starting from the surface of the material and ending at the compound layer/substrate interface. For example, an ε/ε + γ' compound layer is composed of an ε single-phase sublayer adjacent to the surface of the compound layer followed by an ε + γ' dual-phase sublayer adjacent to the ferritic substrate. Note that no specific indication is used for the α-iron substrate.

A. Influence of the Nitriding Potential on the Compound-Layer Evolution; Series A

Nitrocarburizing of pure α-iron substrates at the lowest applied nitriding potential of $r_N = 0.3$ atm$^{-1/2}$ (series A) showed the formation of a closed cementite layer at the surface of the substrate (cf. Figure 1(a)), which is in agreement with the experiments reported in Reference 15. An increased nitriding potential ($r_N = 0.35$ atm$^{-1/2}$) resulted in the development of an inhomogeneous microstructure.** Besides a monophase

---

**Inhomogeneous means that the phase constitution of the microstructure and, thus, the composition in the compound layer varies as function of the lateral position on the specimen cross section. According to the current observations, the position/height of the specimen in the furnace did not influence the distribution of the different microstructures: The linear gas flow rates in the furnace are high enough so that the effective chemical potentials of N and C are constant along the surface of the specimen during the heat treatment.

---

cementite layer adjacent to the surface, a complex dual-phase microstructure of intrinsically nitrogen-poor cementite and nitrogen-richer ε is present in the compound layer (cf. Figures 1(b) and (c)). A reproduction of this experiment ($r_N = 0.35$ atm$^{-1/2}$) resulted again in the formation of an inhomogeneous microstructure showing, at different lateral positions, an $\varepsilon/\varepsilon + \gamma$'double layer (Figure 1(d)) and a θ/ε double layer (Figure 1(e)). At one location, the θ sublayer had transformed into ε in association with a locally increased thickness of the compound layer (dashed arrow in Figure 1(e)). At higher nitriding potentials ($r_N = 0.4$ atm$^{-1/2}$ and $r_N = 0.5$ atm$^{-1/2}$), the microstructure is composed of a laterally homogeneous $\varepsilon/\varepsilon + \gamma$'double layer. In particular, the morphology of the compound layer generated at the highest nitriding potential of $r_N = 0.5$ atm$^{-1/2}$ approaches the well-known morphology of an ε/γ'double layer obtained after pure nitriding (Figure 1(g) and see Reference 33).

Evidently, the previous results reveal a strong effect of the nitriding potential on the microstructural evolution of the compound layer. With increasing nitriding potential ($r_N = 0.3$ atm$^{-1/2}$ to $r_N = 0.5$ atm$^{-1/2}$), corresponding with an increasing content of nitrogen in the compound layer, the microstructure evolves from a carbon-rich and virtually nitrogen-free cementite layer to a nitrogen-rich $\varepsilon/\varepsilon + \gamma$' double layer.

B. Influence of the Treatment Time on the Compound-Layer Evolution; Series B

Nitrocarburizing of pure α-iron substrates as a function of time was performed at 853 K (580 °C) using a nitriding potential of $r_N = 0.35$ atm$^{-1/2}$ (series B), i.e., an intermediate value of r_N with respect to the range of r_N values covered by the experiments of series A (Section III–A). For short treatment times (15 minutes), a closed intrinsically nitrogen-poor cementite layer had developed at the surface of the substrate. Slightly longer nitrocarburizing-times (30 minutes) induced the formation of the nitrogen-richer ε phase in some regions at the cementite/substrate interface leading to the formation of

locally confined θ/ε double-layers. After 2 hours, a laterally inhomogeneous microstructure was obtained: At some locations, the compound layer is composed of a massive cementite layer (Figure 2(a)) that, proceeding laterally, changes to a θ/ε double layer and to a nitrogen-richer $\varepsilon/\varepsilon + \gamma$' double layer (Figure 2(b)). After continued nitrocarburizing (4 hours and 8 hours), the laterally inhomogeneous microstructure of the compound layer reveals an $\varepsilon/\varepsilon + \gamma$' double layer (Figure 2(c)) and also an $\varepsilon + \gamma$' dual-phase layer (Figure 2(d)). After long treatment times (24 hours), the microstructure consisted of an $\varepsilon + \gamma$' dual-phase layer (Figure 2(e)) and also of a single-phase γ' layer (Figure 2(f)).

The preceding results show a complex time dependence of the microstructure of the compound layer. With increasing treatment time, the microstructure evolves from a carbon-rich and virtually nitrogen-free cementite layer to nitrogen-richer $\varepsilon + \gamma$' and γ' layers.

In both series (A and B), the development of the microstructure of the compound layer proceeds from a carbon-rich phase to nitrogen-rich phases. Whereas such a development for series A seems to be linked with an increasing value of the imposed nitriding potential, it is unclear at this stage (but see what follows) why a change in treatment time under constant nitrocarburizing conditions invokes a similar microstructural development for series B.

C. Role of Nitrogen Saturation of the Substrate

An initially nonsaturated, α-iron substrate can become saturated with nitrogen during nitrocarburizing, given sufficient treatment time, i.e., a (very) thin substrate is much faster saturated with nitrogen than a thick substrate (note that the carbon solubility in the α-Fe substrate can be neglected; see Table I). Against this background, wedge-shaped substrates with a linear variation in thickness from 1 mm to 0.02 mm (cf. Section II) were used for nitrocarburizing.

Nitrocarburizing of wedge-shaped α-iron substrates for 4 hours at 853 K (580 °C) (cf. Table II, series C) showed a strong variation in the microstructure of the compound layer as a function of the substrate thickness (Figure 3). After nitrocarburizing, the thick end of the specimen is covered with a massive cementite layer as shown in Figure 3(b) (in agreement with the result for the rectangular 1-mm-thick, nonsaturated substrate nitrocarburized under the same conditions; cf. series A, Figure 1(a)). The formation of nitrogen-richer ε at the cementite layer/substrate interface had occurred close to the thin end of the substrate, i.e., an $\theta/\theta + \varepsilon$ double layer occurs at this location (Figure 3(c)). At the thin end of the substrate, a θ/ε double layer was obtained (Figure 3(d)). Evidently, the amount of ε in the compound layer increases from the thick end to the thin end of the substrate.

Nitrocarburizing of rectangular, 1-mm-thick, nonsaturated and nitrogen pre-saturated α-iron substrates for 4 hours at 853 K (580 °C) (cf. Table II, series C) led to the formation of strikingly dissimilar microstructures of the compound layer. After nitrocarburizing of the nonsaturated substrate, a single-phase θ layer was obtained (Figure 4(a) and see Figure 1(a)), whereas after nitrocarburizing of the nitrogen presaturated
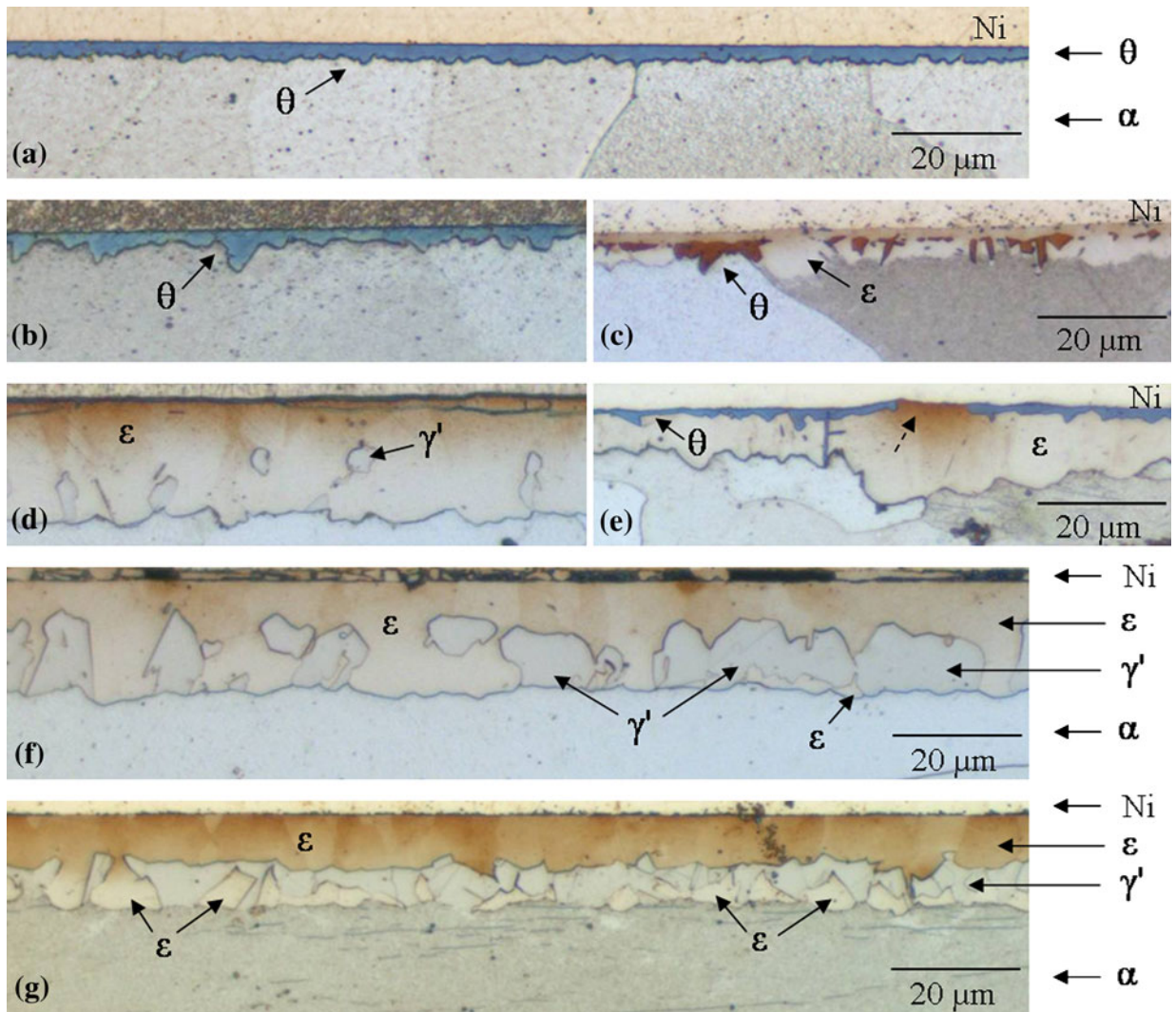
Fig. 1—Optical micrographs showing cross sections (after etching with 1 vol pct Nital containing 0.1 vol pct HCl and staining with an alkaline potassium permanganate solution) of compound layers grown on α-Fe substrates by nitrocarburizing for 4 h at 853 K (580 °C) for various nitriding potentials (series A): (a) cementite layer, $r_N = 0.30$ atm$^{-1/2}$; (b) to (c) massive cementite layer and $\varepsilon/\theta + \varepsilon$ double layer, $r_N = 0.35$ atm$^{-1/2}$; (d) to (e) $\varepsilon/\varepsilon + \gamma'$ double layer and θ/ε double layer, $r_N = 0.35$ atm$^{-1/2}$. The dashed arrow in (e) indicates transformation of the θ sublayer into ε phase; (f) $\varepsilon/\varepsilon + \gamma'$ double layer, $r_N = 0.4$ atm$^{-1/2}$; (g) $\varepsilon/\varepsilon + \gamma'$ double layer, $r_N = 0.5$ atm$^{-1/2}$.

substrate, a θ/ε double layer had developed (Figure 4(b)). The corresponding X-ray diffraction patterns are given in Figure 5.

To determine the degree of nitrogen saturation in the α-iron substrate, in relation to the specific microstructure of the compound layer on top of the substrate, hardness measurements were performed in the diffusion zone, at positions laterally apart, directly underneath the compound layer, with a microstructure that varied from a carbon-rich cementite single layer to a nitrogen-rich $\varepsilon/ \varepsilon + \gamma'$ double-layer (cf. Figures 2(a) and (b); rectangular specimen nitrocarburized in an 15.44 pct NH$_3$, 57.95 pct H$_2$, 20 pct CO, and 6.61 pct N$_2$ gas mixture; series B). The results are shown in Figure 6; the local nitrogen concentration in the ferrite substrate was calculated from the measured hardness values as described in Section II. The hardness measurements show that in the ferrite substrate underneath the compound layer, where ε is present in the microstruc-

ture, a nitrogen content of approximately 0.35 at. pct occurs, which is practically equal to the nitrogen-solubility limit in ferrite at 853 K (580 °C) of approximately 0.36 at. pct.[17] Underneath the massive cementite layer, a remarkably lower nitrogen content of 0.25 at. pct occurs in the ferrite substrate. The lower nitrogen content underneath the cementite layer can be ascribed to an inhibited diffusion of nitrogen through cementite compared with the diffusion of nitrogen through iron (carbo)nitrides.[23,32,34]

IV. DISCUSSION

A. Kinetics: Origin of the Microstructural Evolution of the Compound Layer

As will be demonstrated in the following discussion, the time-dependent (series B) and atmosphere-dependent (series A) evolutions of the microstructure of the
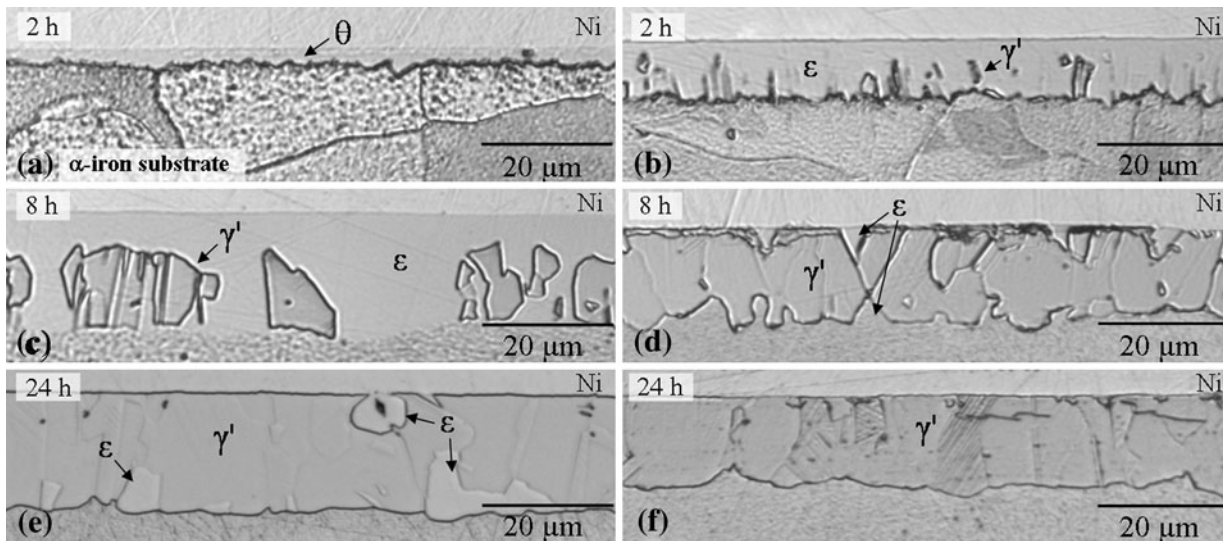
Fig. 2—Optical micrographs showing cross sections (after etching with 1 vol pct Nital containing 0.1 vol pct HCl) of compound layers grown on α-Fe substrates by nitrocarburizing for various treatment times at 853 K (580 °C) (series B): (a) to (b) cementite layer and $\varepsilon/\varepsilon + \gamma'$ double layer obtained after 2 h, (c) to (d) $\varepsilon/\varepsilon + \gamma'$ double layer and $\varepsilon + \gamma'$ dual-phase layer obtained after 8 h, and (e) to (f) $\varepsilon + \gamma'$ layer and γ' layer obtained after 24 h.

compound layer can be explained by assuming that local equilibria prevail at the solid–solid phase interfaces, whereas solid–gas equilibrium does not necessarily prevail at the surface of the compound layer. The time-dependent microstructural evolution of the compound layer can be caused by (1) the finite rates of nitrogen and carbon transfer from the gas phase to the α-Fe substrate (before and after compound-layer formation) and (2) the finite thickness of the plate-like specimens used in the current experiments, implying a gradual saturation of the initially unsaturated substrate after nitrocarburizing. As a consequence, in the case of a gas atmosphere of constant composition, the microstructure of the compound layer will evolve as function of treatment time.[†] In the current case, the characteristic

---

[†]A time-invariant phase constitution (microstructure) of the compound layer is expected to occur only for the case of a constant nitrogen and carbon concentration at the surface of the compound layer (implying local equilibrium or stationary state at the gas–solid interface) in combination with (1) a nitrogen and carbon saturated substrate or (2) an infinitely thick substrate with initially constant nitrogen and carbon content. In such cases (and assuming local equilibrium at the solid–solid interfaces in the compound layer), the so-called Boltzmann transformation can be applied to Fick's second law, implying a time-invariant diffusion path (lateral gross composition as a function of depth) and a parabolic growth of the compound-layer thickness.[4,7,35]

---

evolution of phases in the compound layer can be described as a consequence of the large difference of the solubilities of nitrogen and carbon in the α-iron substrate (see Figure 7(b)) that affects the local solid–solid equilibrium at the compound layer/substrate interface. As shown in the Fe-N-C phase diagram at 853 K (580 °C) (Figure 7(b)), the α-iron single-phase field exhibits a maximum solubility of 0.36 at. pct for

nitrogen and of 0.018 at. pct for carbon,[17] i.e., both solubilities differ by a factor of 20.

The phase *changes* observed at the surface of the compound layer as function of time (series B, Figure 2) indicate that *at the surface*, no "local equilibrium" occurs between the gas phase and the solid phase, at least not for short and intermediate treatment times, which is discussed subsequently.

The uptake of nitrogen and carbon from the nitrocarburizing gas atmosphere in the ferrite substrate is controlled by (1) the rate of NH$_3$ and CO dissociation (possibly catalyzed) at the substrate surface, leading to adsorbed nitrogen and carbon atoms, (2) the rate of recombination (and possibly desorption) of the adsorbed atoms, and (3) the diffusion rates of, subsequently absorbed, nitrogen and carbon in the substrate away from the surface. Finite values for the nitrogen and carbon uptake imply that a local equilibrium,[‡] as

---

[‡]For example, if the recombination and desorption of adsorbed nitrogen atoms from the specimen surface cannot be neglected compared with the rate of NH$_3$ dissociation, a stationary state instead of a local equilibrium occurs, i.e., the chemical potential of nitrogen in the solid at the surface of the specimen is lower than that pertaining to the nitrocarburizing atmosphere.[12,36]

---

prescribed by the chemical potentials of nitrogen and carbon, as pertaining to the composition of the nitrocarburizing atmosphere, cannot be established at once (i.e., at t = 0).

The rate of carbon transfer from CO gas to ferrite has been found to be much faster than the rate of nitrogen transfer from NH$_3$ gas.[37] It can be concluded that the relatively low solubility of carbon in ferrite (cf. Table I) in combination with the relatively fast uptake of carbon (recognizing that the diffusivities of carbon and nitrogen
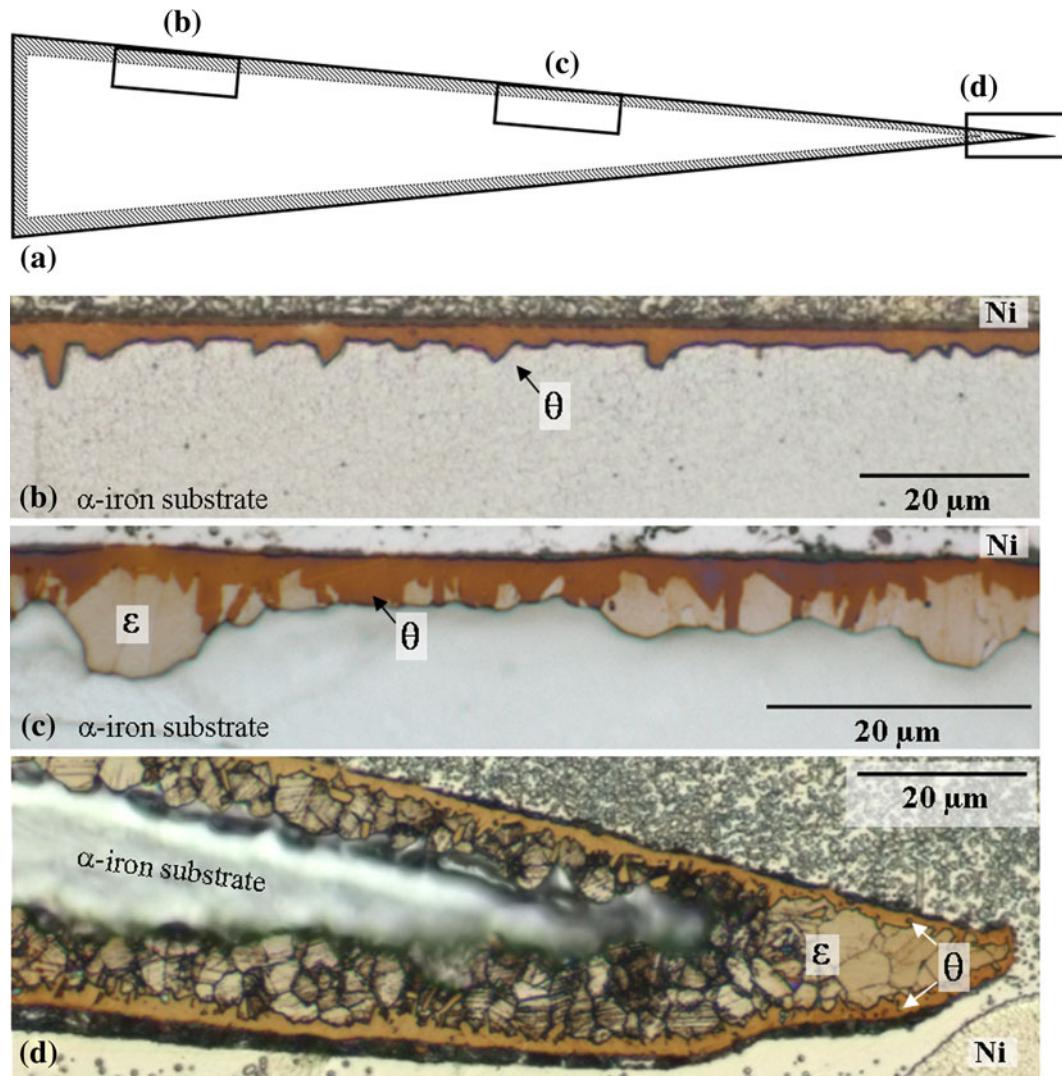
Fig. 3—Optical micrographs showing cross sections (after etching with 1 vol pct Nital containing 0.1 vol pct HCl and staining with an alkaline potassium permanganate solution) of compound layers obtained on a wedge-shaped α–iron specimen by nitrocarburizing for 4 h at 853 K (580 °C) using a 13.23 vol pct NH_3, 57.95 vol pct H_2, 20 vol pct CO, 8.82 vol pct N_2, (r_N = 0.30 $atm^{-1/2}$) gas mixture: (*a*) schematic illustration of the wedge-shaped specimen showing the lateral positions of the optical micrographs shown in (*b*) to (*d*); (*b*) cementite layer at the thick end of the sample; (*c*) $\theta/\theta + \varepsilon$ double layer close to the thin end of the sample; and (*d*) θ/ε double layer at the thin end of the sample.

in α-iron do not differ much[38]) causes the ferrite substrate to be much faster saturated with carbon than with nitrogen at the early stage of nitrocarburizing.§

---

§Even in the case of finite but about equal transfer rates of nitrogen and carbon, the solubility limit of carbon will be surpassed first as a consequence of the large difference of the solubility limits of nitrogen and carbon.

Hence, at the surface of the substrate, the initial formation of nitrogen-poor cementite instead of a nitrogen-richer (carbo)nitride can occur (Figure 7(b), point A), although the presence of the latter phase at the surface would comply with thermodynamic equilibrium with the gas atmosphere or with the establishment of a stationary state (see footnote‡), as suggested by the phase constitution at the surface of the compound layer after long treatment times (cf. Section III–B). The first

observation and interpretation along these lines for the initial formation of cementite was presented in References 22 and 23.

After continued nitrocarburizing, the surface-adjacent region of the substrate becomes enriched with nitrogen gradually by the continuous diffusion of nitrogen through (the grain boundaries of) the cementite layer as discussed in detail in Reference 32. The nucleation of ε at the cementite layer/substrate interface is then induced if the nitrogen concentration in ferrite at the layer/substrate interface exceeds a critical value (Figure 7(b), point B): First, a local equilibrium of θ, ε, and α and then, after further nitrogen enrichment of the substrate, a local equilibrium of α and ε, prevails. Note that ε can be formed also by the conversion of cementite, as demonstrated first in Reference 39.

The role of the substrate saturation with nitrogen on the microstructural evolution of the compound layer is supported fully by the results obtained from the
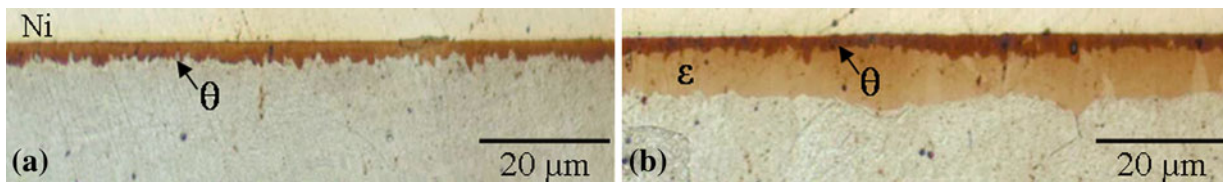
Fig. 4—Optical micrographs (after etching with 1 vol pct Nital containing 0.1 vol pct HCl and staining with an alkaline potassium permanganate solution) showing cross-sections of compound layers obtained by nitrocarburizing for 4 h at 853 K (580 °C) using a 13.23 vol pct NH$_3$, 57.95 vol pct H$_2$, 20 vol pct CO, 8.82 vol pct N$_2$ (r_N = 0.30 atm$^{-1/2}$) gas mixture. (*a*) Cementite layer grown on a pure α-iron substrate. (*b*) θ/ε double layer grown on a nitrogen presaturated α-iron substrate.
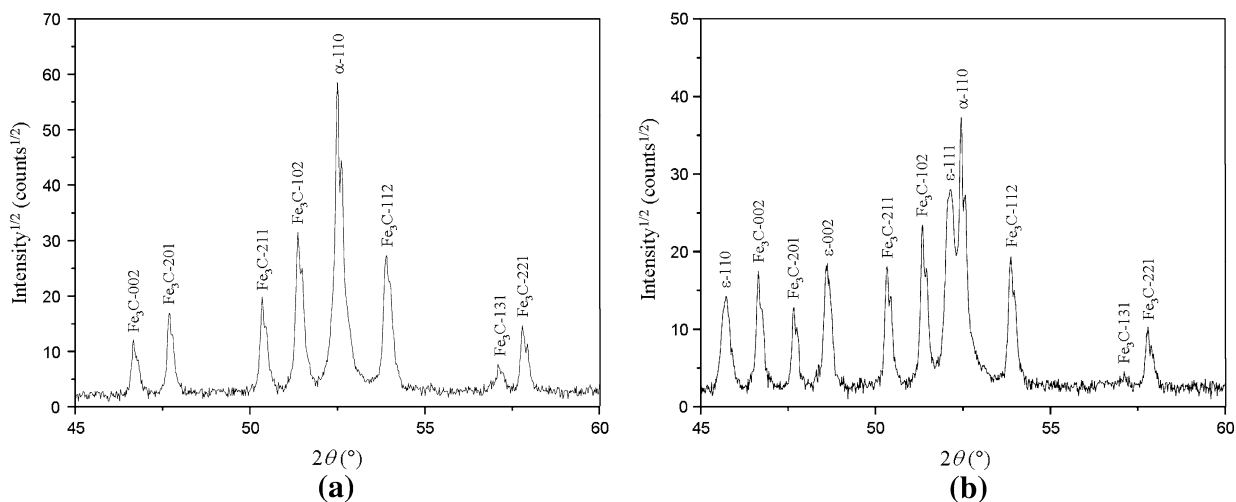

Fig. 5—Exemplary X-ray diffraction patterns (Co-K$_\alpha$ radiation) of compound layers obtained by nitrocarburizing for 4 h at 853 K (580 °C) using a 13.23 vol pct NH$_3$, 57.95 vol pct H$_2$, 20 vol pct CO, 8.82 vol pct N$_2$, (r_N = 0.30 atm$^{-1/2}$) gas mixture. (*a*) Cementite layer grown on a pure α-iron substrate (cf. Fig. 4(a)), (*b*) θ/ε double layer grown on a nitrogen presaturated α-iron substrate (cf. Fig. 4(b)).

wedge-shaped specimens (series C; Figure 3) nitrocarburized under conditions where (initially) pure cementite layers were obtained on the usual, 1-mm-thick, rectangular ferrite substrates (see series A). Indeed, at the thick end of the wedge-shaped specimen, the substrate was not saturated with nitrogen after nitrocarburizing, which led to the formation of a single-phase cementite layer. At some distance away, toward the thin end (rim) of the specimen, nitrogen saturation of the substrate was reached resulting in the development of a θ + ε dual-phase layer adjacent to the substrate. At the thin end (rim) of the specimen, the substrate was saturated fast with nitrogen resulting in the formation of a θ/ε double layer (Section IV–C).

The effect of nitrogen saturation on the development of the microstructure of the compound layer is also confirmed by nitrocarburizing of a nonsaturated, rectangular specimen and a nitrogen presaturated, rectangular specimen using a strongly carburizing atmosphere (series C; Figure 4). The nonsaturated substrate showed the formation of a massive cementite layer, whereas a θ/ε double layer had developed on the nitrogen presaturated substrate.

The hardness measurements in the ferrite underneath a laterally inhomogeneous (θ/ε and ε/θ + ε) compound layer (cf. series B, Section III–C; Figure 6) show that the formation of ε–(carbo)nitride occurs only at locations of the layer/substrate interface where the substrate is

(practically) saturated with nitrogen (for more details, see Section IV–C).

Based on the preceding discussion, the occurrence of similar stages in the compound-layer evolution of series A (variable gas composition with constant treatment time; Section III–A) compared with series B (variable treatment time with constant gas composition; Section III–B) can now be understood as well: The substrate becomes faster saturated with nitrogen after applying a higher nitriding potential (cf. series A and cf. Figures 1 and 2).

B. Thermodynamics: Microstructure and Diffusion Paths Within the Compound Layer

As described subsequently, the observed phase constitution and interphase boundaries *within* the compound layer are in agreement with the metastable§§

---

§§"Metastable" because θ, ε, and γ' are considered not to decompose into graphite, nitrogen gas, and α-Fe as required for "stable" phase equilibria.

---

ternary Fe-N-C phase diagram at 853 K (580 °C),[16,17,40,41] *i.e.,* "local equilibria" prevail at the interphase boundaries in the compound layer. As a preparation for this discussion, the observations on the
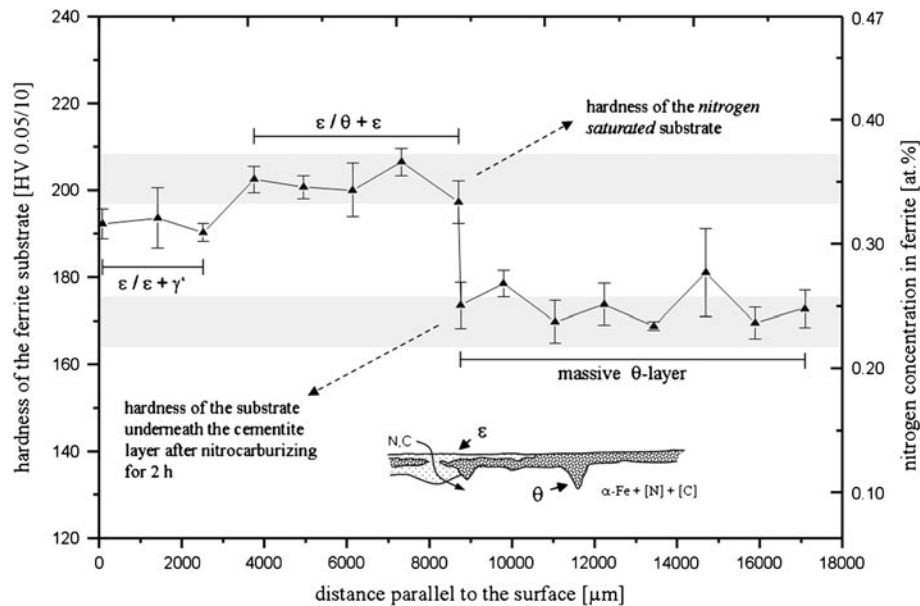
Fig. 6—Vickers hardness and the corresponding nitrogen concentration in the ferrite substrate directly underneath the laterally inhomogeneous compound layer obtained after nitrocarburizing using the following process parameters: 15.44 pct NH_3, 57.95 pct H_2, 20 pct CO, 6.61 pct N_2 ($r_N = 0.35$ atm$^{-1/2}$), 2 h, and 853 K (580 °C). For the inset in the bottom part of this figure, see the discussion of Fig. 9.

time-dependent development of the microstructure have been summarized schematically in Figure 8.

After the initial formation of a single-phase θ layer at the surface (stage 1), the subsequent formation of ε at the cementite layer/substrate interface occurs and results in either a θ/ε (stage 2a) double layer or a $\theta/\theta + \varepsilon$ double layer (stage 2b). Then, the amount of ε in the compound layer increases strongly by the growth of ε into the substrate and the simultaneous conversion of cementite into ε[¶] at the surface-adjacent region of the compound

---

[¶]The possible conversion of cementite into ε was first reported in Reference 39 after nitriding of pearlitic substrates at 843 K (570 °C).

---

layer (stages 3 and 4), for which the development ends with the presence of a single-phase ε layer (stage 5). Next, the γ' phase is formed at the interface between the ε layer and the substrate leading to an $\varepsilon/\varepsilon + \gamma'$ double layer (stages 6a and 6b) and then to an ε/γ' double layer (stage 7). The final stage of the compound layer development involves increasing the amount of γ' until a single-phase γ' layer results (stage 8). The occasional formation of an $\varepsilon + \gamma'$ dual-phase layer (Figures 2(d) and (e)) is not considered in Figure 8 as a separate stage. It should be recognized that the single stages can overlap in time, as indicated by the laterally inhomogeneous nature of the microstructure of the compound layer (cf. Figures 1 and 2, and Section IV–C).

In the final stage of compound-layer evolution, a single-phase γ' layer is obtained (Figure 2(f) and stage 8 in Figure 8). The γ'-phase can contain only little carbon because of its narrow composition range (Table I). So the question emerges, where the appreciable amount carbon taken up initially in the compound layer has gone. The uptake of carbon by the α-iron substrate can be excluded because of the small solubility limit of

carbon in ferrite[¶¶] (see Table I). It is concluded that the

---

[¶¶]Moreover, as shown in Figure 7, the formation of a single-phase γ' layer from a cementite and/or an ε containing compound layer is possible only if the carbon content in the α-iron substrate at the layer/substrate interface is decreased.

---

carbon has escaped through the surface into the gas atmosphere.

Now, starting from the phase at the surface of the compound layer and its composition and ending at the α-iron substrate, different diffusion paths, representing the change of the lateral gross composition and phase constitution of the compound layer as function of depth at constant time, can be indicated schematically in the isothermal section of the ternary Fe-N-C phase diagram at 853 K (580 °C) for different stages of compound-layer growth. With reference to Figure 8, proposals of these diffusion paths have been made in Figure 7(a); observe the full lines with arrows (if possible the diffusion paths were simplified by straight lines). The time-dependent change in the microstructure of the compound layer implies that the diffusion path changes correspondingly during nitrocarburizing. It follows that the microstructural development as observed within the compound layer can be understood as a straightforward consequence of (1) the depth dependence of the gross composition at the stage of nitrocarburizing considered and (2) the thermodynamics of the Fe-N-C system, determining the solid–solid local equilibria. Consequently, kinetic constraints have not to be invoked to explain the microstructure within the compound layer.

A coexistence of cementite and γ' (i.e., cementite being directly in contact with γ' as reported for a temperature of 823 K [550 °C] in Reference 15) was never observed in the current study pertaining to a temperature of
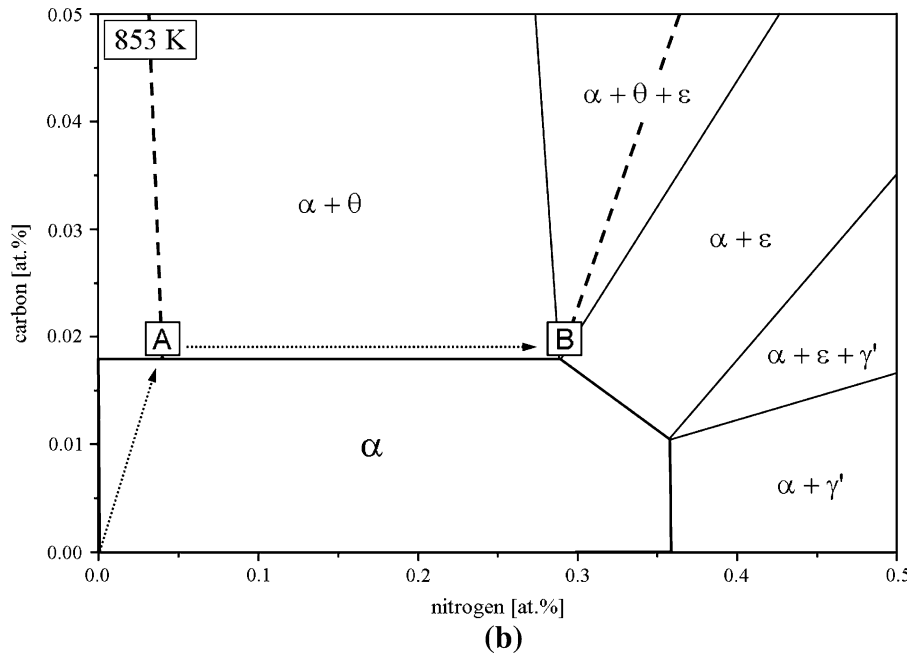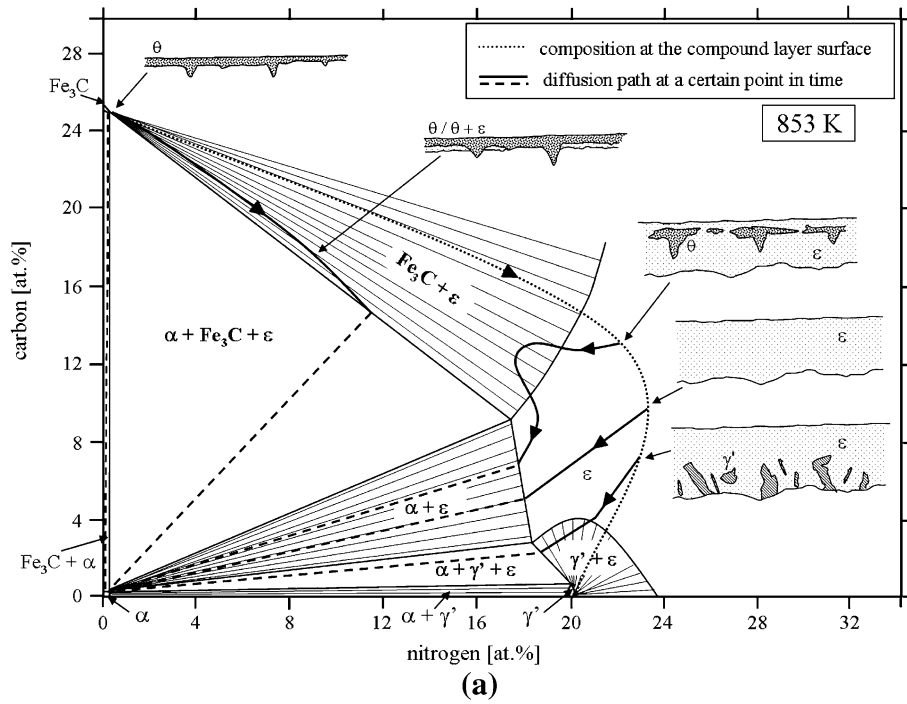
(a)

(b)

Fig. 7—Isothermal section of the metastable Fe-N-C phase diagram at 853 K (580 °C). The time-dependent microstructural evolution of the compound layer from carbon-rich to nitrogen-rich phases after nitrocarburizing at 853 K (580 °C) is illustrated schematically by diffusion paths featuring, at a given time, the phase constitution and the lateral gross composition from the top to the bottom of the compound layer (solid lines with arrows for continuously changing gross composition, dashed lines for jumps in gross composition). (*a*) Isothermal section with phase boundaries according to Reference 24 (The invariant transition reaction γ' + Fe₃C → α + ε was found to occur at a (single) temperature in the range between 833 K an 843 K (560 °C to 570 °C), as determined by a series of experiments in Reference 24. However, according to calculations based on the CALPHAD database (2008), the invariant transition reaction α + γ' + ε → γ would occur between 848 K and 853 K (575 °C and 580 °C), which is not in agreement with Reference 24 and with the observed evolution of the compound-layer microstructure.) showing the entire relevant range of composition. (*b*) The time-dependent change of the gross composition at the surface is indicated by a dotted line with arrows. The iron-rich corner of the isothermal section shows the phase boundaries of the α-iron single-phase field.[17] The time-dependent change of the nitrogen and carbon content in the ferrite substrate at the surface and subsequently at the layer (cementite)/substrate (ferrite) interface after nitrocarburizing has been indicated schematically by the dotted lines with arrows. For the points A and B, see the text. Within the α phase, the diffusion path is not shown because the starting point (substrate surface) and the end point (substrate center) of the diffusion path change with time.
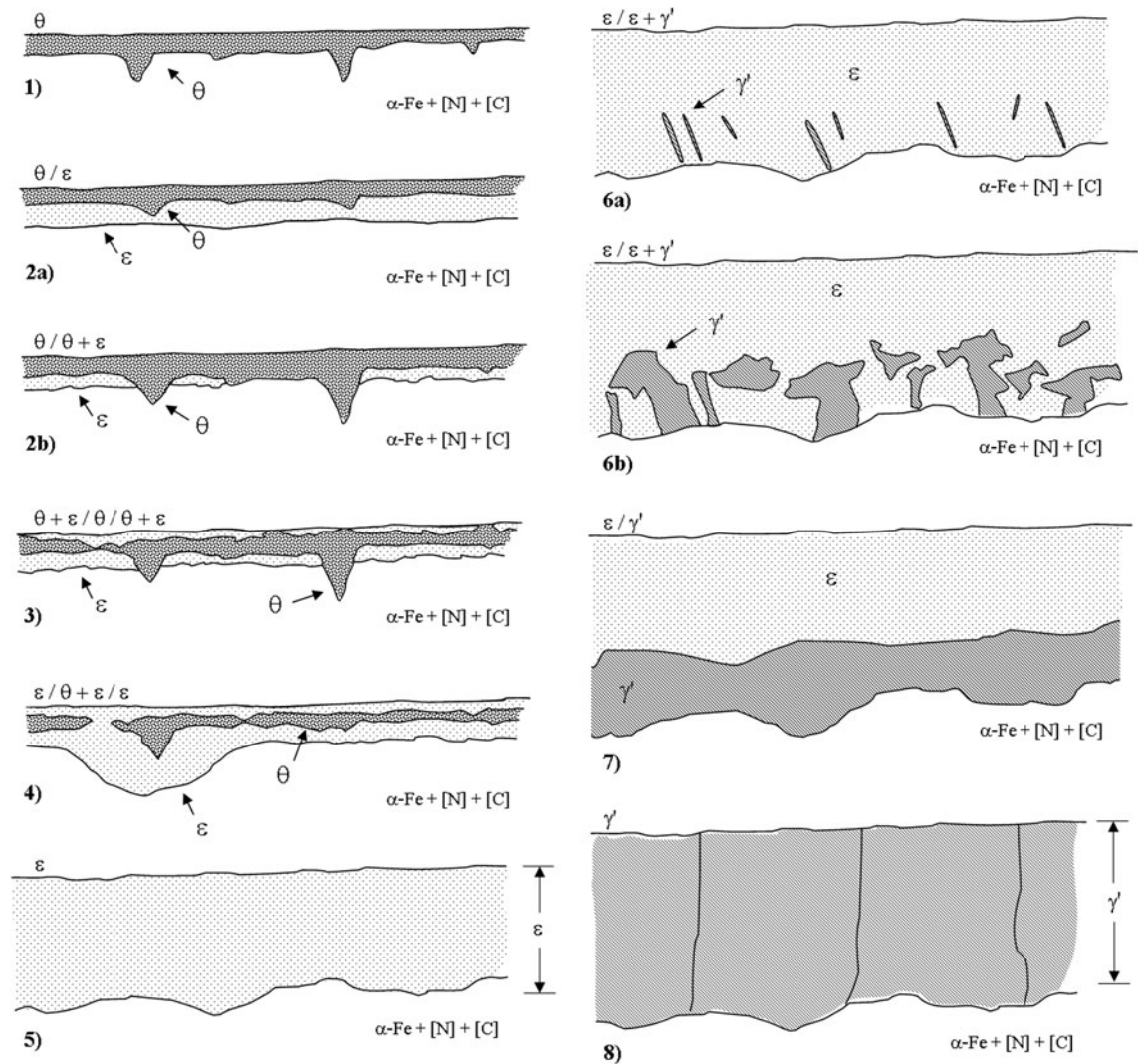
Fig. 8—Schematic illustration of the progressive microstructural stages of the compound-layer evolution on pure α-iron as function of time upon nitrocarburizing at 853 K (580 °C). The development starts with the occurrence of a carbon-rich phase and proceeds toward nitrogen-rich phases along diffusion paths compatible with the Fe-N-C phase diagram; see Fig. 7(a). (1) single-phase θ layer, (2a) θ/ε double layer, (2b) $\theta/\theta + \varepsilon$ layer, (3) $\theta + \varepsilon/\theta/\theta + \varepsilon$ double layer, (4) $\varepsilon/\theta + \varepsilon/\varepsilon$ layer, (5) single-phase ε layer, (6a) ε with some γ' developing at regions close to the compound layer/substrate interface, (6b) $\varepsilon/\varepsilon + \gamma$' double layer, (7) ε/γ' double layer, and (8) single-phase γ' layer.

853 K (580 °C). This finding is in agreement with the ternary Fe-N-C phase diagram[17,24] where a two-phase field of cementite and γ' does not exist at 853 K (580 °C) (cf. Figure 7(a)). The two-phase equilibrium $\alpha + \varepsilon$ obtained in the microstructure of the compound layer after nitrocarburizing of nitrogen presaturated substrates (series C; cf. Figure 4(b)) indicates clearly the temperature of 853 K (580 °C) to be above the single temperature for the invariant reaction $\theta + \gamma' \rightarrow \varepsilon + \alpha$ in the Fe-N-C system, which is consistent with experimental results reported in Reference 24, where this temperature has been claimed to lie in the range of 833 K to 843 K (560 °C to 570 °C).

C. Kinetics: Origin of Lateral Inhomogeneity of the Microstructure of the Compound Layer

Apart from the thermodynamically prescribed multiphase nature of the compound layer (see the preceding discussion and the diffusion paths in Figure 7(a)), a lateral inhomogeneity of the microstructure is induced by the dramatic increase in the diffusive flux of

---

*The diffusional flux of carbon into the α-iron substrate can be neglected because of the small solubility limit of carbon in ferrite; see Table I.

---

nitrogen* through the compound layer at those regions, where the initially formed cementite layer has already been locally transformed into the ε phase. Nitrogen diffusion through cementite (formed in the first stage of nitrocarburizing) might vary locally depending on the local microstructure (e.g., the local presence of an initially high grain-boundary density might enhance the local flux of nitrogen through the cementite layer; cf. Reference 26). Consequently, along the θ/α interface, a variation occurs for the time needed to attain the critical
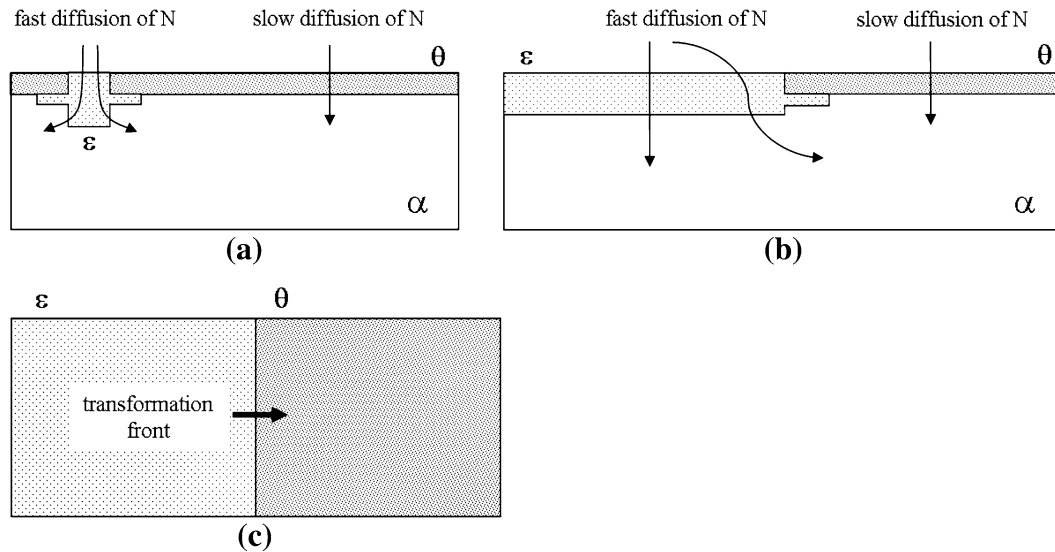
Fig. 9—Schematic illustration of a mechanism enhancing the lateral inhomogeneity of the microstructure of the compound layer. (*a*) Cross-sectional view of the compound layer showing fast diffusion of nitrogen through ε at locations where the initially formed cementite layer has been converted locally into ε (the diffusion of nitrogen through cementite is comparably slow[32]). A diffusional carbon flux in the ferrite substrate is neglected because of the small carbon solubility in ferrite. (*b*) Following the short-circuit diffusion illustrated in (a) and (b), the lateral diffusion of nitrogen underneath the cementite layer leads to a lateral saturation of the substrate at the θ/ε transformation front and, thus, to the subsequent formation of ε, *i.e.*, the θ/ε transformation front proceeds laterally at the specimen surface. (*c*) Top view of the specimen shown in (b).

concentration of nitrogen in the substrate for the formation of ε at the θ/α interface (cf. point B in Figure 7(b)). After prolonged nitrocarburizing, this ε might grow from the θ/α interface through cementite to the surface of the compound layer. The growth of the ε phase might occur additionally by the conversion of θ into ε at the surface of the compound layer because of the gradually increasing chemical potential of nitrogen at the surface (cf. the discussion in Section IV–A). Because the diffusivity of nitrogen through ε is much higher than through cementite, "short-circuit diffusion" of nitrogen through an ε "channel" becomes possible (cf. Figure 9(a), dashed arrow in Figure 1(e)). Such a nitrogen short-circuit diffusion, followed by a lateral diffusion of nitrogen through ε and α underneath the cementite layer, will result in a laterally proceeding saturation of the substrate with nitrogen at the transformation front between θ and ε (cf. Figure 6). This mechanism contributes to a laterally proceeding transformation of the cementite layer into an ε-rich compound layer (cf. Figure 9(b) and (c), and see Figures 1(b) through (e), 2(a) through (d)). The (local) development of the ε phase at the surface of the compound layer can be observed macroscopically because the reflectivity of the cementite phase regions at the surface is higher than that of the ε phase regions.

It is noted that the thickness of the compound layer depends on the amount of cementite in the microstructure: cementite acts as a barrier for the inward diffusion of nitrogen and carbon, in particular compared with the ε phase.[9,15,23,32,33,42] Indeed, a retarded growth of the overall compound layer and, thus, a smaller compound-layer thickness was observed (also locally) for microstructures exhibiting (also locally) a high amount of cementite.

V. CONCLUSIONS

1. The microstructural evolution of the compound layer developing after nitrocarburizing of α-iron starts with the formation of carbon-rich cementite and develops into the direction of the nitrogen-richer and carbon-poorer phases ε and γ'.
2. Local equilibrium (or stationary state) conditions do not necessarily prevail at the gas–solid interface, at least not in the beginning of nitrocarburizing.
3. The initial formation of cementite and the subsequent formation of ε are the consequence of (1) a solubility of nitrogen in α-iron much larger than that of carbon and (2) a rate of nitrogen transfer from the gas phase into the solid much lower than that of carbon, *i.e.*, kinetics governs the developing composition and phase constitution *at* the gas–solid and compound layer–substrate interfaces.
4. Cementite acts as barrier for the inward diffusion of nitrogen. This leads to a retarded growth of the compound layer at locations where cementite is present, as well as initiates the lateral inhomogeneity of the microstructure as a consequence of "short-circuit" diffusion of nitrogen through ε "channels" traversing the originally closed cementite layers.
5. Local equilibrium conditions *do* prevail within the compound layer at solid–solid phase boundaries. The change of the microstructure (phase constitution and lateral gross composition) as a function of depth in the compound layer is compatible with so-called "diffusion paths" in the ternary Fe-N-C phase diagram, *i.e.*, thermodynamics governs the microstructure *within* the compound layer. The use of diffusion paths is a powerful method to visualize

the relation between the microstructure of the compound layer and (the isothermal section of) the corresponding phase diagram.

6. The courses of microstructural change of the compound layer as observed after increasing the treatment time at a constant gas composition and as observed after increasing the nitriding potential at a constant treatment time are identical.

7. A two-phase equilibrium $\varepsilon + \alpha$ occurs in the Fe-N-C system at 853 K (580 °C) as validated by the formation of θ/ε double layers on top of nitrogen presaturated α-iron substrates.

ACKNOWLEDGMENT

REFERENCES

1. F.J.J. Van Loo, M.R. Rijnders, K.J. Ronka, J.H. Gulpen, and A.A. Kodentsov: *Solid State Ionics*, 1997, vol. 95 (1–2), pp. 95–106.
2. P.M. Unterweiser: *Source Book on Nitriding*, ASM, Materials Park, OH, 1977.
3. A.A. Kodentsov, G.F. Bastin, and F.J.J. Van Loo: *J. Alloys Compd.*, 2001, vol. 320, pp. 207–17.
4. F.J.J. Van Loo: *Progr. Solid State Chem.*, 1990, vol. 20, pp. 47–99.
5. J.M.G. Vilar and J.M. Rubí: *Proc. Natl. Acad. Sci. U S A*, 2001, vol. 98, pp. 11081–84.
6. Y.H. Sohn and M.A. Dayananda: *Acta Mater.*, 2000, vol. 48, pp. 1427–33.
7. J.S. Kirkaldy and D.J. Young: *Diffusion in the Condensated State*, The Institute of Metals, London, U.K., 1987.
8. G. Ghosh: *J. Electron. Mater.*, 1998, vol. 27, pp. 1154–60.
9. M.A.J. Somers: *Heat Treat. Met.*, 2000, vol. 4, pp. 92–102.
10. J. Slycke: *Nitrieren und Nitrocarburieren*, AWT, Darmstadt, Germany, 1996, pp. 19–28.
11. M.A.J. Somers and E.J. Mittemeijer: *Surf. Eng.*, 1987, vol. 3, pp. 123–37.
12. E.J. Mittemeijer and M.A.J. Somers: *Surf. Eng.*, 1997, vol. 13, pp. 483–37.
13. P.F. Colijn, E.J. Mittemeijer, and H.C.F. Rozendaal: *Z. Metallkd.*, 1983, vol. 74, pp. 620–27.
14. J. Slycke and L. Sproge: *Surf. Eng.*, 1989, vol. 5, pp. 125–40.
15. T. Gressmann, M. Nikolussi, A. Leineweber, and E.J. Mittemeijer: *Scripta Mater.*, 2006, vol. 55, pp. 723–26.
16. H. Du: *J. Phase Equil.*, 1993, vol. 14, pp. 682–93.
17. J. Kunze: *Nitrogen and Carbon in Iron and Steel*, Akademie-Verlag Berlin, Germany, 1990.
18. T. Bell: *Heat Treat. Met.*, 1975, vol. 2, pp. 39–49.
19. C. Dawes and D.F. Tranter: *Heat Treat. Met.*, 1985, vol. 3, pp. 70–76.
20. T. Bell and D.H. Thomas: *Metall. Trans. A*, 1979, vol. 10A, pp. 79–84.
21. E.J. Mittemeijer: *J. Heat Treat.*, 1983, vol. 3, pp. 114–19.
22. M.A.J. Somers, P.F. Colijn, W.G. Sloof, and E.J. Mittemeijer: *Z. Metallkd.*, 1990, vol. 81, pp. 33–43.
23. H. Du, M.A.J. Somers, and J. Ågren: *Metall. Mater. Trans. A* 2000, vol. 31A, pp. 195–211, 801.
24. M. Nikolussi, A. Leineweber, E. Bischoff, and E.J. Mittemeijer: *Int. J. Mater. Res.*, 2007, vol. 98, pp. 1086–92.
25. T. Woehrle, A. Leineweber, and E.J. Mittemeijer: *HTM J. Heat Treat. Mater.*, 2010, vol. 65, pp. 243–48.
26. M. Nikolussi, A. Leineweber, and E.J. Mittemeijer: *J. Mater. Sci.*, 2009, vol. 44, pp. 770–77.
27. E. Lehrer: *Z. Elektrochem.*, 1930, vol. 36, pp. 383–92.
28. S.S. Hosmani, R.E. Schacherl, and E.J. Mittemeijer: *Acta Mater.*, 2006, vol. 54, pp. 2783–92.
29. H.A. Wriedt, N.A. Gokcen, and R.H. Nafziger: *Bull. Alloy. Phase. Diagr.*, 1987, vol. 8, pp. 355–77.
30. A. Wells: *J. Mater. Sci.*, 1985, vol. 20, pp. 2439–45.
31. G. Petzow: *Metallographic Etching*, ASM International, Materials Park, OH, 1999.
32. M. Nikolussi, A. Leineweber, and E.J. Mittemeijer: *Phil. Mag.*, 2010, vol. 90, pp. 1105–22.
33. M.A.J. Somers and E.J. Mittemeijer: *Metall. Mater. Trans. A*, 1995, vol. 26A, pp. 57–74.
34. T. Sone, E. Tsunasawa, and K. Yamanaka: *Trans. Japan Inst. Met.*, 1981, vol. 22, pp. 237–43.
35. J. Crank: *The Mathematics of Diffusion*, Oxford Science Publications, Oxford, U.K., 1975.
36. E.J. Mittemeijer and J.T. Slycke: *Heat Treat. Met.*, 1996, vol. 3, pp. 67–71.
37. H.J. Grabke: *Archiv Eisenhütten.*, 1975, vol. 46, pp. 75–81.
38. M. Weller: *Mater. Sci. Forum*, 2001, vols. 366–368, p. 95.
39. E.J. Mittemeijer, W.T.M. Straver, P.F. Colijn, P.J. van der Schaaf, and J.A. van der Hoeven: *Scripta Metall.*, 1980, vol. 14, pp. 1189–92.
40. J. Kunze: *Härterei-Tech. Mitt.*, 1996, vol. 51, pp. 348–55.
41. J. Slycke, L. Sproge, and J. Ågren: *Scand. J. Metall.*, 1988, vol. 17, pp. 122–26.
42. H. Du and J. Ågren: *Z. Metallkd.*, 1995, vol. 86, pp. 522–29.